

**Beamlike photon-pair generation for two-photon interference and polarization entanglement**Hsin-Pin Lo,<sup>1,2</sup> Atsushi Yabushita,<sup>2</sup> Chih-Wei Luo,<sup>2</sup> Pochung Chen,<sup>1</sup> and Takayoshi Kobayashi<sup>2,3,4,5</sup><sup>1</sup>*Department of Physics, National Tsing Hua University, Hsinchu, 300, Taiwan, Republic of China*<sup>2</sup>*Department of Electrophysics, National Chiao-Tung University, Hsinchu, 300, Taiwan, Republic of China*<sup>3</sup>*International Cooperative Research Project, Japan Science and Technology Agency, 4-1-8 Honcho, Kawaguchi, Saitama 332-0012, Japan*<sup>4</sup>*University of Electro-Communications, 1-5-1 Chofugaoka, Chofu, Tokyo 182-8585, Japan*<sup>5</sup>*Institute of Laser Engineering, Osaka University, 2-6 Yamada oka, Suita, Osaka 565-0971, Japan*

(Received 25 October 2010; published 14 February 2011)

Beamlike photon pairs were generated by spontaneous parametric down-conversion using a type-II  $\beta$ -BaB<sub>2</sub>O<sub>4</sub> crystal. A pump laser generated photon pairs when it transmitted through the crystal and was reflected back into the crystal by a mirror to generate more photon pairs. The photon pairs generated when the pump laser first transmitted through the crystal (first photon pairs) were also reflected back into the crystal to overlap with the light path of the photon pairs generated in the second transmission of the pump laser through the crystal (second photon pairs). We observed interference between the first and second photon pairs modulated with a half period of the wavelength of the photon pairs, which demonstrates two-photon interference using the beamlike photon pairs. The fringe period confirms that the observed interference is not classical interference but quantum two-photon interference. Through rotating the angles of quarter-wave plates in the light paths of the photon pairs, we generated beamlike photon pairs with entangled polarization. The phase between the first and second photon pairs could be tuned by changing the position of mirrors reflecting the pump pulses and photon pairs. The fringes of coincidence counts showed that the beamlike photon pairs have polarization entanglement.

DOI: [10.1103/PhysRevA.83.022313](https://doi.org/10.1103/PhysRevA.83.022313)

PACS number(s): 03.67.Bg, 03.65.Ud

**I. INTRODUCTION**

Spontaneous parametric down-conversion (SPDC) has been used to generate photon pairs entangled in various parameters. Polarization-entangled photon pairs have been utilized for quantum information experiments, like quantum teleportation and quantum key distribution [1]. Wave vector entanglement of the photon pairs has demonstrated quantum imaging [2,3], photonic de Broglie wavelength measurement [4–6], two-photon interference [7,8], and quantum lithography [9–11]. Nonlocal pulse shaping [12] and spectroscopy [13] have been performed by frequency-entangled photon pairs. Generally, a polarization-entangled photon pair is generated by using a type-II  $\beta$ -BaB<sub>2</sub>O<sub>4</sub> (BBO) crystal, which generates a horizontally polarized photon and a vertically polarized photon as a pair. Figure 1(a) shows a schematic graph of the photon-pair generation, in which two different colored light cones have differently polarized photons. The CCD image of the observed photon pairs is shown in Fig. 1(b). Photon pairs are polarization entangled only at crossing points of the light cones; therefore the polarization-entangled photon pairs could be obtained by using a spatial filter to block other photons, which do not pass through the crossing points. The spatial filtering results in low production efficiency of the polarization-entangled photon pairs.

By adjusting the angle of the BBO crystal, beamlike photon pairs [14] can be generated as shown in Fig. 1(c). Figure 1(d) shows a CCD image of the generated photon pairs. In previous work by Ou *et al.* [15], the polarization-entangled beamlike photon pairs were generated by using two type-II BBO crystals. In this work, we developed a scheme to generate beamlike photon pairs, which demonstrate two-photon interference and polarization entanglement. The scheme was experimentally verified by showing the measurement results. Additionally, by rotating the angles of quarter-wave plates in the light paths of

photon pairs, we could also generate polarization-entangled beamlike photon pairs.

**II. EXPERIMENT**

The schematic drawing of our experimental setup is shown in Figs. 2(a) and 2(b). A Ti:sapphire oscillator (Spectra-Physics, model Tsunami, 1.4 W, 100 fs, 80 MHz at 800 nm) was used to pump a frequency doubler unit (Spectra-Physics, model 3980-4) and generated a second-harmonic (SH) signal of 470 mW. The SH beam pumped a 2-mm-thick type-II BBO crystal to generate photon pairs via the SPDC process. Each photon pair consists of two photons whose polarizations are orthogonal to each other. For the sake of convenience, the photon in each photon pair that comes out closer to the optical axis is called the signal photon ( $S_1$ ) in this paper. The other one is called the idler photon ( $I_1$ ). Generally, the signal and idler photons of the SPDC pairs are emitted conically from a point on the BBO crystal illuminated by the pump beam [see Fig. 1(a)]. In this work, the angle of the crystal was adjusted to generate beamlike photon pairs as shown in Fig. 1(c).

The mirrors  $M_S$  and  $M_I$  reflected the signal photons ( $S_1$ ) and idler photons ( $I_1$ ), respectively, to pass through the point where the BBO crystal is illuminated by the reflected pump beam. A mirror  $M_P$  reflected the pump beam to illuminate the BBO crystal and also generate photon pairs whose signal photon and idler photon were expressed as  $S_2$  and  $I_2$ , respectively. Adjustment of mirror  $M_S$  ( $M_I$ ) made the optical path of  $S_1$  ( $I_1$ ) overlap that of  $S_2$  ( $I_2$ ). The coincidence of  $S_1$  and  $I_1$  and that of  $S_2$  and  $I_2$  were measured using a pair of single-photon counting modules (PerkinElmer, SPCM-AQR-14) and a time-to-amplitude converter (ORTEC, model 567).

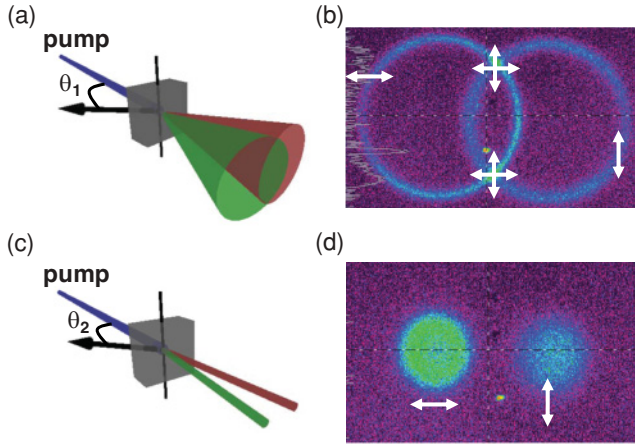


FIG. 1. (Color online) (a) and (c) The SPDC light cones when they are overlapped and beamlike, respectively. Arrows show the optical axis of the nonlinear crystal. (b) and (d) The CCD images of the SPDC light cones of (a) and (c), respectively.

### III. RESULTS AND DISCUSSION

#### A. Hong-Ou-Mandel (HOM) dip measurements for path length adjustment

Figure 2(a) shows the setup for the measurement of the HOM dip. The fiber couplers  $FC_S$  and  $FC_I$  were connected to a single-mode  $2 \times 2$  fiber (Thorlabs, FC830-50B-FC) whose other ends were connected to single-photon counting modules. A half-wave plate (HWP) was inserted in front of  $FC_I$  to rotate the polarizations of the idler photons ( $I_1$  and  $I_2$ )  $90^\circ$ . This made the polarization of the idler photons ( $I_1$  and  $I_2$ ) parallel with that of the signal photons ( $S_1$  and  $S_2$ ) in the  $2 \times 2$  fiber.

Scanning the position of  $FC_S$  along the optical path of the signal photons, we observed a HOM dip to identify the coincidence of  $S_2$  and  $I_2$  by blocking the light paths of  $S_1$  and  $I_1$  [16]. The width of the HOM dip shows the coherence length of the signal-idler fields  $\ell_{\text{coh}}$ , which corresponds to the inverse of the bandwidth of interference filters (Semrock: LL01-780-25, 3 nm) put in front of  $FC_S$  and  $FC_I$ . The path length from the BBO crystal to  $FC_S$  and that to  $FC_I$  were set to be equal by fixing the position of  $FC_S$  at the bottom of the HOM dip. Blocking the pump beam in front of the mirror  $M_P$ , a HOM dip was observed by scanning the position of the mirror  $M_S$  along the optical path of the signal photon. The HOM dip obtained by scanning  $M_S$  is shown in Fig. 3 for reference. The path length from the BBO crystal to  $M_S$  and that to  $M_I$  were also equalized by fixing the position of  $M_S$  at the bottom of the observed HOM dip.

#### B. Two-photon interference of beamlike photon pairs

Figure 2(b) shows the setup used for the two-photon interference measurements. We have fixed the positions of  $FC_S$  and  $M_S$  at the bottoms of the HOM dips as described in the previous section. A quarter-wave plate  $QWP_S$  was inserted between the BBO crystal and the mirror  $M_S$ . In the optical path between the BBO crystal and the mirror  $M_I$ , another quarter-wave plate  $QWP_I$  was inserted. The angles of the quarter-wave plates  $QWP_S$  and  $QWP_I$  were set to preserve the original polarizations of the photons  $S_1$  and  $I_1$ , respectively.

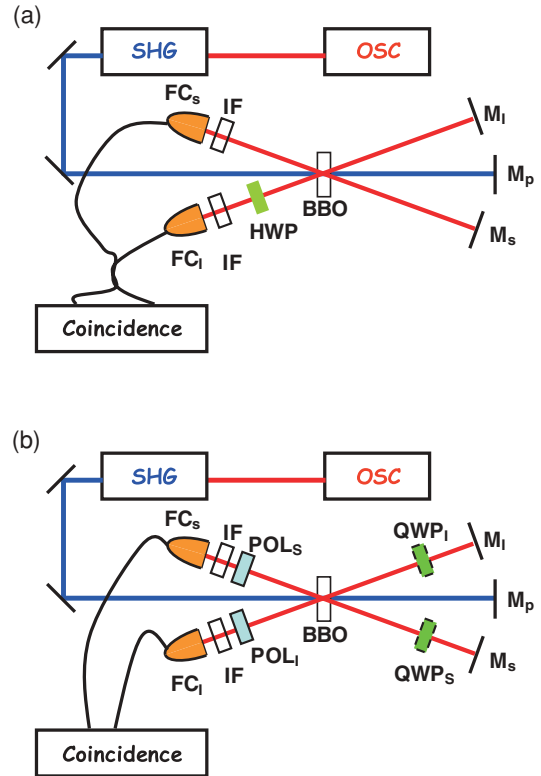


FIG. 2. (Color online) (a) Schematic drawing of the measurement of HOM dip. (b) Schematic drawing of the measurement of two-photon interference and polarization entanglement. OSC, oscillator; SHG, second-harmonic generator (frequency doubler); Coincidence, coincidence counting unit;  $M_i$ , mirror; BBO,  $\beta$ -BaB<sub>2</sub>O<sub>4</sub> crystal;  $POL_i$ , polarizer; IF, interference filter;  $FC_i$ , fiber coupler; HWP, half-wave plate;  $QWP_i$ , quarter-wave plate ( $i = I, S$ ).

Therefore, the polarization of  $S_1$  ( $I_1$ ) is the same as that of  $S_2$  ( $I_2$ ). The polarizers  $POL_S$  and  $POL_I$  were inserted in front of the photon counters,  $FC_S$  and  $FC_I$ , respectively. The angle of  $POL_S$  ( $POL_I$ ) was set to transmit the photon that has polarization of the signal (idler) photons.

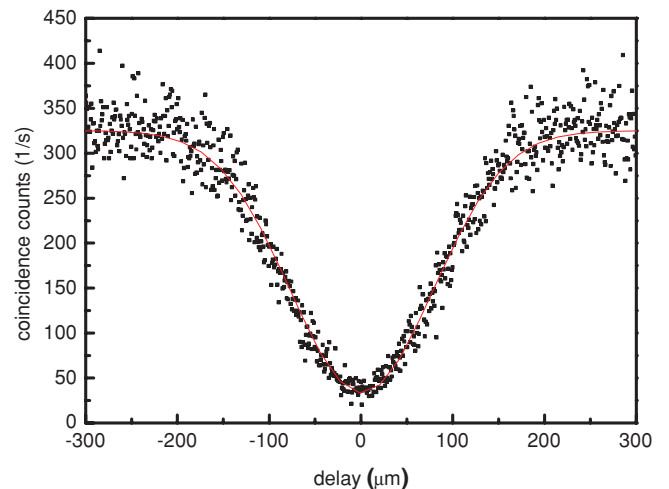


FIG. 3. (Color online) Hong-Ou-Mandel interference measurement result, which was observed by scanning the position of mirror  $M_S$ . Curves are the fitting results.

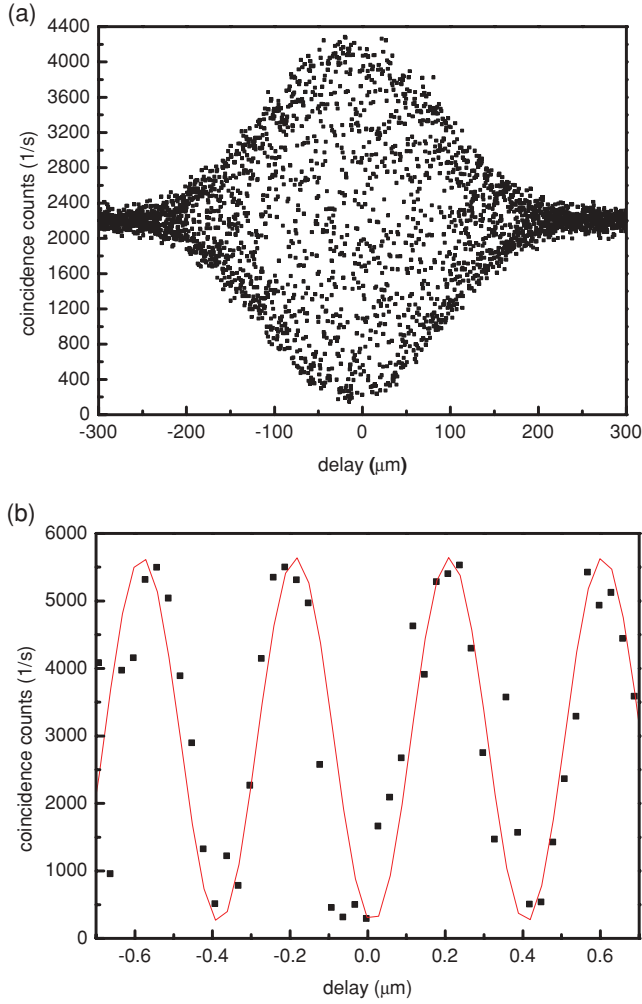


FIG. 4. (Color online) (a) Coincidence count rate observed by scanning the position of  $M_P$ . The result shows an envelope of a Gaussian function reflecting the coherence length of the pump beam. (b) Center part of (a) magnified to show the fringe period clearly. Curves are the fitting results.

The coincidence of  $S_1$  and  $I_1$  and that of  $S_2$  and  $I_2$  were observed by scanning the position of the mirror  $M_P$ . Figures 4(a) and 4(b) show the observed coincidence count  $R_C$ , which shows fringes appearing at a period of pump wavelength (390 nm). The fringe period certifies that the observed fringe reflects the two-photon interference between the first photon pair ( $S_1$  and  $I_1$ ) and the second photon pair ( $S_2$  and  $I_2$ ). The envelope of the fringes shows a Gaussian dependence whose width reflects the coherent length of the pump beam. The reason the fringe has a period of 390 nm with a Gaussian envelope can be explained as follows in an analogy of the work reported by Boyd *et al.* [17]. The two-photon interference can be explained in terms of the superposition of two-photon probability amplitudes [18,19]. Figure 5 represents the schematic diagram of the two-photon interference using two-photon path diagrams [20,21]. Alternatives 1 and 2 are the SPDC pathways for the first photon pair ( $S_1$  and  $I_1$ ) and the second photon pair ( $S_2$  and  $I_2$ ). The pump pulse was assumed to have a Gaussian spectrum with a coherence length  $\ell_{\text{coh}}^P$  whose spectrum width is much narrower than those of the signal and

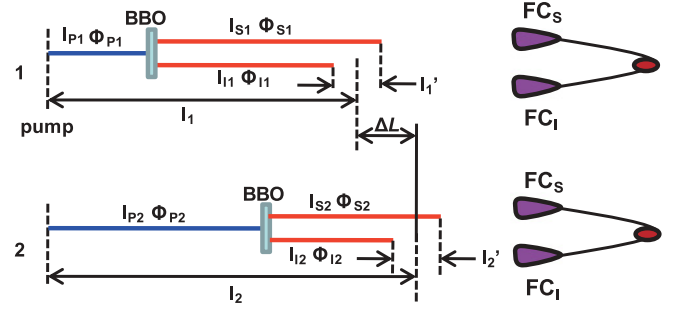


FIG. 5. (Color online) Schematic diagram of the two-photon interference. Alternatives 1 and 2 are the two pathways for the photon-pair generation.

idler fields. In Fig. 4 the subscripts  $P$ ,  $S$ , and  $I$  represent pump, signal, and idler, respectively. The optical path length traveled by a photon is expressed by the parameter  $l$ , and  $\phi$  denotes the phase other than the dynamical one, such as phase modulation caused by reflections, a geometric phase [18,22]. The biphoton path length  $l_i$  and the biphoton path-asymmetry length  $l'_i$  for  $i$  ( $i = 1, 2$ ) can be defined as

$$l_i = \frac{l_{S_i} + l_{I_i}}{2}, \quad (1)$$

$$l'_i = l_{S_i} - l_{I_i}.$$

The differences in the biphoton path lengths, the biphoton path-asymmetry lengths, and the phase between the alternatives 1 and 2 are denoted as  $\Delta L$ ,  $\Delta L'$ , and  $\Delta\phi$ , respectively, and calculated as follows:

$$\Delta L \equiv l_1 - l_2 = \left( \frac{l_{S1} + l_{I1}}{2} + l_{P1} \right) - \left( \frac{l_{S2} + l_{I2}}{2} + l_{P2} \right),$$

$$\Delta L' \equiv l'_1 - l'_2 = (l_{S1} - l_{I1}) - (l_{S2} - l_{I2}), \quad (2)$$

$$\Delta\phi \equiv (\phi_{S1} + \phi_{I1} + \phi_{P1}) - (\phi_{S2} + \phi_{I2} + \phi_{P2}).$$

Generalizing the calculation of Refs. [23,24], the coincidence count rate of the photon pairs  $R_C$  can be calculated as

$$R_C \propto 1 + \gamma(\Delta L) \gamma'(\Delta L') \times \cos \left[ k_{P0} \Delta L + \left( \frac{k_{S0} - k_{I0}}{2} \right) \Delta L' + \Delta\phi \right]. \quad (3)$$

Here  $k_{i0}$  stands for the mean vacuum wave vector magnitude of the pump wave ( $i = P$ ), signal wave ( $i = S$ ), and idler wave ( $i = I$ ).  $\gamma(\Delta L)$  and  $\gamma'(\Delta L')$  are normalized correlation functions of the pump and the signal-idler fields, calculated as  $\gamma(\Delta L) = \exp[-\frac{1}{2}(\Delta L/\ell_{\text{coh}}^P)^2]$  and  $\gamma'(\Delta L') = \exp[-\frac{1}{2}(\Delta L'/\ell_{\text{coh}})^2]$ .

The positions of  $FC_S$  and  $M_S$  were set to satisfy  $l_{S1} = l_{I1}$  and  $l_{S2} = l_{I2}$ , which results in  $\Delta L' = 0$ . Therefore, the coincidence rate shown in Eq. (3) can be simplified as

$$R_C \propto 1 + \gamma(\Delta L) \cos[k_{P0} \Delta L + \Delta\phi]. \quad (4)$$

The first term in the cosine function  $k_{P0} \Delta L$  explains why the measured coincidence count rate showed the fringe in the period of the pump wavelength as shown in Fig. 4(b).

The Gaussian envelope of the observed fringes reflects the coefficient  $\gamma(\Delta L)$  multiplied by the cosine function in Eq. (4).

### C. Polarization entanglement of beamlike photon pairs

The first photon pair ( $S_1$  and  $I_1$ ) and the second photon pair ( $S_2$  and  $I_2$ ) are beamlike photon pairs, and they overlap with each other as described in the previous sections. When  $\Delta L$  and  $\Delta L'$  are much smaller than  $l_{\text{coh}}^P$  and  $l_{\text{coh}}$ , respectively, the normalized correlation functions  $\gamma(\Delta L)$  and  $\gamma'(\Delta L')$  are near unity, and the quantum state of the overlapped beamlike photon pairs can be written as

$$|\Psi\rangle = |H\rangle_S |V\rangle_I + \exp\left\{i\left[phk_{p0}\Delta L + \left(\frac{k_{s0} - k_{I0}}{2}\right)\Delta L' + \Delta\phi\right]\right\} |H\rangle_S |V\rangle_I. \quad (5)$$

After the measurement of the two-photon interference, the quarter-wave plates (QWP<sub>S</sub> and QWP<sub>I</sub>) were rotated 45° in the setup shown in Fig. 2(b). Passing through the quarter-wave plates twice, each photon of the first photon pair ( $S_1$  and  $I_1$ ) is rotated 90° in its polarization. This makes the polarization of  $S_1$  ( $I_1$ ) orthogonal to that of  $S_2$  ( $I_2$ ). Therefore, the spatial overlap of the optical path between the first photon pair and second photon pair makes the overlapped beamlike photon pairs entangled in their polarizations. The following equation shows the quantum state of the polarization-entangled beamlike photon pair:

$$|\Psi\rangle = |V\rangle_S |H\rangle_I + \exp\left\{i\left[phk_{p0}\Delta L + \left(\frac{k_{s0} - k_{I0}}{2}\right)\Delta L' + \Delta\phi\right]\right\} |H\rangle_S |V\rangle_I. \quad (6)$$

Here, we define linearly polarized states  $|+\rangle = \frac{1}{\sqrt{2}}(|H\rangle + |V\rangle)$  and  $|-\rangle = \frac{1}{\sqrt{2}}(|H\rangle - |V\rangle)$ . Using  $|+\rangle$  and  $|-\rangle$ , Eq. (6) can be written as

$$|\Psi\rangle = \frac{1}{2}(1 + e^{i\Phi})(|+\rangle_S |+\rangle_I - |-\rangle_S |-\rangle_I) + \frac{1}{2}(1 - e^{i\Phi})(|+\rangle_S |-\rangle_I - |-\rangle_S |+\rangle_I), \quad (7)$$

$$\Phi = k_{p0}\Delta L + \left(\frac{phk_{s0} - k_{I0}}{2}\right)\Delta L' + \Delta\phi. \quad (8)$$

The following equation shows the coincidence count rate of  $|+\rangle_S |-\rangle_I$ :

$$R_{+-} \propto |\langle\Psi|+\rangle_S |-\rangle_I|^2 = |1 - e^{i\Phi}|^2 = 2(1 - \cos\Phi). \quad (9)$$

When the mirror  $M_P$  is scanned,  $\Delta L$  changes while the values of  $\Delta L'$  and  $\Delta\phi$  are kept. Therefore, Eqs. (8) and (9) show that  $R_{+-}$  is expected to be modulated at the period of the pump wavelength when the mirror  $M_P$  is moved. Its experimental confirmation was demonstrated as follows.

The angles of the polarizers POL<sub>S</sub> and POL<sub>I</sub> are adjusted to pass photons of  $|+\rangle_S \langle +|_S$  and  $|-\rangle_I \langle -|_I$ , respectively. Then the coincidence count rate of the photon pair was measured, scanning the position of the mirror  $M_P$ . The measured result is shown in Figs. 6(a) and 6(b). Figure 6(b) shows a larger statistical error than Fig. 5(b). The reason is thought to be that

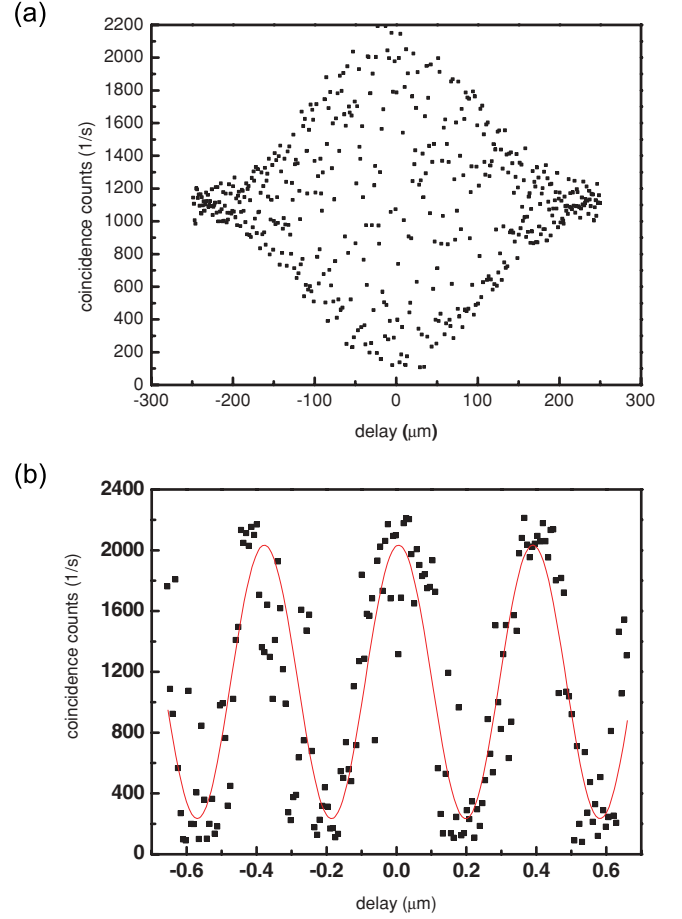


FIG. 6. (Color online) (a) Coincidence count rate observed by scanning the position of  $M_P$ . The result shows an envelope of a Gaussian function reflecting the coherence length of the pump beam. (b) Center part of (a) magnified to show the fringe period clearly. Curves are the fitting results.

the coincidence count rate in Fig. 6(b) is smaller than that in Fig. 5(b); therefore the data in Fig. 6(b) are more sensitive to noise than in Fig. 5(b). The result clearly shows that the coincidence rate is modulated with the period of the pump wavelength of 390 nm. Visibility of the fringe is thought to reflect the entanglement of the generated state, which is explained below.

The entanglement  $E(\Psi)$  can be calculated by following the process explained in [25]:

$$E(\Psi) = h\left(\frac{1 + \sqrt{1 - C^2}}{2}\right), \quad (10)$$

$$h(x) = -x \log_2 x - (1 - x) \log_2 (1 - x), \quad (11)$$

$$C(\Psi) = |\langle\Psi|(\sigma_y \otimes \sigma_y)|\Psi^*\rangle|. \quad (12)$$

Here,  $\sigma_y$  is the Pauli matrix,

$$\sigma_y = \begin{pmatrix} 0 & -i \\ i & 0 \end{pmatrix}. \quad (13)$$

When the state is maximally and minimally entangled,  $E(\Psi)$  is unity and zero, respectively.  $E(\Psi)$  monotonically increases and ranges from 0 to 1 as  $C$  goes from 0 to 1, so one can take the concurrence as a measure of entanglement. From Eqs. (6)

[or (7)] and (12) the concurrence is given by  $C = |\cos\Phi|$ . The visibility of the coincidence count rate  $R_{+-}$  shown in Fig. 6 was estimated to be  $0.90 \pm 0.05$ . Considering Eq. (9) and  $C = |\cos\Phi|$ , maximum concurrence obtained in the present work was estimated to be  $0.90 \pm 0.05$ .

#### IV. CONCLUSION

In this work we have developed a scheme to generate beamlike photon pairs for two-photon interference and polarization entanglement. The pump beam generated a photon pair (first photon pair). The pump beam remaining after generation of the first photon pair was reflected back into the BBO crystal to generate another photon pair (second photon pair). The initially generated photon pair was reflected back to let its optical path overlap the optical path of the second photon pair.

When the optics was configured for the two-photon interference, we observed a fringe modulated at the period of the wavelength of the pump laser. This corresponds to the quantum two-photon interference between the initially generated photon pair and the second photon pair.

By rotation of the quarter-wave plates, the setup generated beamlike photon pairs that are entangled in polarization. The coincidence count of  $|+\rangle_S|-\rangle_I$  was observed by scanning the position of the mirror  $M_P$ , and the result showed the fringe, which is also modulated at the period of the pumping wavelength. The concurrence of the pair was calculated to be  $0.90 \pm 0.05$ , which defines the degree of entanglement of the generated photon pairs. This confirms that the generated beamlike photon pair is highly entangled in its polarization.

#### ACKNOWLEDGMENTS

This work was supported by the National Science Council of the Republic of China, Taiwan (Grant No. NSC 98-2112-M-009-001-MY3); a grant from the Ministry of Education, Aiming for Top University (MOE ATU) Program at National Chiao-Tung University (NCTU); and the International Cooperative Research Project (ICORP) program of the Japan Science and Technology Agency (JST).

- 
- [1] W. Tittel and G. Weihs, *Quantum Inf. Comput.* **1**, 3 (2001).
  - [2] Y. H. Shih, *J. Mod. Opt.* **49**, 2275 (2002).
  - [3] T. B. Pittman, Y. H. Shih, D. V. Strekalov, and A. V. Sergienko, *Phys. Rev. A* **52**, R3429 (1995).
  - [4] E. J. S. Fonseca, C. H. Monken, and S. Pádua, *Phys. Rev. Lett.* **82**, 2868 (1999).
  - [5] J. Jacobson, G. Björk, I. Chuang, and Y. Yamamoto, *Phys. Rev. Lett.* **74**, 4835 (1995).
  - [6] K. Edamatsu, R. Shimizu, and T. Itoh, *Phys. Rev. Lett.* **89**, 213601 (2002).
  - [7] D. V. Strekalov, A. V. Sergienko, D. N. Klyshko, and Y. H. Shih, *Phys. Rev. Lett.* **74**, 3600 (1995).
  - [8] C. K. Hong, Z. Y. Ou, and L. Mandel, *Phys. Rev. Lett.* **59**, 2044 (1987).
  - [9] M. D'Angelo, M. V. Chekhova, and Y. H. Shih, *Phys. Rev. Lett.* **87**, 013602 (2001).
  - [10] R. Shimizu, K. Edamatsu, and T. Itoh, *Phys. Rev. A* **67**, 041805 (2003).
  - [11] A. N. Boto, P. Kok, D. S. Abrams, S. L. Braunstein, C. P. Williams, and J. P. Dowling, *Phys. Rev. Lett.* **85**, 2733 (2000).
  - [12] M. Bellini, F. Marin, S. Viciani, A. Zavatta, and F. T. Arecchi, *Phys. Rev. Lett.* **90**, 043602 (2003).
  - [13] A. Yabushita and T. Kobayashi, *Phys. Rev. A* **69**, 013806 (2004).
  - [14] S. Takeuchi, *Opt. Lett.* **26**, 843 (2001).
  - [15] X-L. Niu, Y-F. Huang, G-Y. Xiang, G-C. Guo, and Z. Y. Ou, *Opt. Lett.* **33**, 968 (2008).
  - [16] C. K. Hong, Z. Y. Ou, and L. Mandel, *Phys. Rev. Lett.* **59**, 2044 (1987).
  - [17] A. K. Jha, M. N. O'Sullivan, Kam Wai Clifford Chan, and R. W. Boyd, *Phys. Rev. A* **77**, 021801(R) (2008).
  - [18] R. J. Glauber, *Phys. Rev.* **130**, 2529 (1963).
  - [19] M. H. Rubin, D. N. Klyshko, Y. H. Shih, and A. V. Sergienko, *Phys. Rev. A* **50**, 5122 (1994).
  - [20] T. B. Pittman, D. V. Strekalov, A. Migdall, M. H. Rubin, A. V. Sergienko, and Y. H. Shih, *Phys. Rev. Lett.* **77**, 1917 (1996).
  - [21] D. V. Strekalov, T. B. Pittman, and Y. H. Shih, *Phys. Rev. A* **57**, 567 (1998).
  - [22] R. Bhandari and J. Samuel, *Phys. Rev. Lett.* **60**, 1211 (1988).
  - [23] Z. Y. Ou, L. J. Wang, and L. Mandel, *Phys. Rev. A* **40**, 1428 (1989).
  - [24] L. J. Wang, X. Y. Zou, and L. Mandel, *Phys. Rev. A* **44**, 4614 (1991).
  - [25] W. K. Wootters, *Phys. Rev. Lett.* **80**, 2245 (1998).